Journal of Applied Physics

RESEARCH ARTICLE | APRIL 15 2026

Cavity-mediated charging of scalable quantum battery based on superconducting flux qubits

Jiadong Shi ; Jiaxu Wu ; Tao Wu

J. Appl. Phys. 139, 154401 (2026)
https://doi.org/10.1063/5.0315566

AIP Publishing

Journal of Applied Physics ARTICLE pubs.aip.org/aip/jap

Cavity-mediated charging of scalable quantum battery based on superconducting flux qubits

Cite as: J. Appl. Phys. **139**, 154401 (2026); doi: 10.1063/5.0315566
Submitted: 13 December 2025 · Accepted: 15 March 2026 ·
Published Online: 15 April 2026

Jiadong Shi,[1,2] Jiaxu Wu,[2] and Tao Wu[2,a)]

AFFILIATIONS

[1]School of Electronic and Information Engineering, Hefei Institute of Technology, Hefei 238076, China
[2]School of Physics and Electronics Engineering, Fuyang Normal University, Fuyang 236037, China

[a)]**Author to whom correspondence should be addressed:** wutaofuyang@126.com

ABSTRACT

By utilizing superconducting flux qubits (FQs) embedded in a transmission line resonator cavity, we propose a scalable quantum battery (QB) and analyze its charging dynamics in the dispersive regime. The QB can be efficiently charged mediated by the cavity, which induces coherence among all FQs through a common photonic mode. Our results indicate that such coherence enhances the charging power. Furthermore, we identify a trade-off: increasing the battery size improves the charging power but reduces the storage capacity. By selecting an appropriate battery size, we achieve a practical QB that combines high power with large capacity. This optimal size can be moderately increased at the cost of a weaker coupling strength between the FQs and the cavity. This work, which integrates superconducting quantum circuits with energy storage technology, may pave the way for scalable and reliable quantum applications.

I. INTRODUCTION

With the development and miniaturization of electronic technologies, the demand for energy storage devices capable of delivering high power density is ever-increasing. In this context, developing strategies to store energy consumed by quantum devices, wherein quantum effects genuinely arise from intrinsic quantum fluctuations, has emerged as a fundamental challenge. Coherence is recognized as one of the most fundamental features of quantum theory, distinguishing the quantum realm from the classical one.[1] Consequently, it is essential to account for the non-trivial quantum phenomena[2,3] that govern the behavior of such quantum components, in regimes where classical thermodynamics breaks down.[4] As a result, quantum thermodynamics was established.[5–7] Compared with its classical counterpart, the most distinctive feature of quantum thermodynamics is the speedup of energy transfer,[8,9] rooted in the fact that quantum effects can typically enhance the performance of classical protocols, i.e., by accelerating underlying dynamics processes.[10] Recently, considerable attention has been devoted to applications of quantum thermodynamics, particularly to exploring how precise control and experimentally implementable operations affect work extraction.[11–13] It has been demonstrated that the quantum Otto engine cycle can be effectively accelerated using shortcut-to-adiabaticity techniques.[14,15]

A quantum battery (QB), defined as a mechanical system that is used to temporarily store energy in quantum degrees of freedom, was initially introduced by Alicki and Fannes.[16] With the advancement of quantum technology, QBs have gradually emerged as a prominent research area. Theoretical progress in this field encompasses the establishment of charging models,[17–19] the exploration of open QB systems,[20–23] and the study of many-body QBs,[24–26] among others. Subsequently, numerous promising experiments on QBs have been carried out using organic microcavities,[27–29] superconducting circuits,[30] quantum dots,[31] and Nuclear Magnetic Resonance (NMR) platforms.[32] To date, considerable research efforts have been dedicated to maximizing the stored energy, minimizing the charging time, or maximizing the average charging power. In practical applications, an ideal QB is expected not only to deliver high power but also to store a significant amount of energy. This gives rise to the following question: is it possible to realize a QB that can simultaneously achieve both high power and large capacity? As is well known, superconducting quantum circuits,[33–36] a promising platform for quantum computation, offer an experimentally viable implementation of

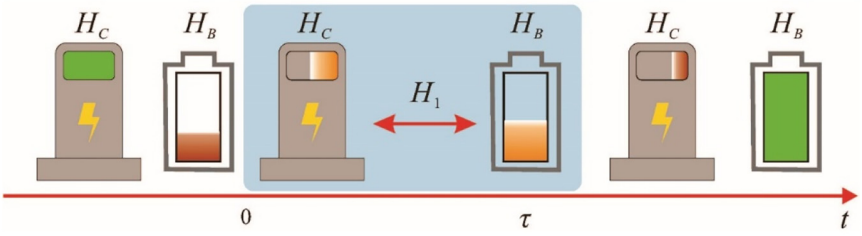

FIG. 1. Schematic representation of the charging protocol. Energy flows from the charger (characterized by Hamiltonian H_C) to the battery (characterized by Hamiltonian H_B). At time $t < 0$, no interaction exists between the two subsystems. During the time interval $0 < t < \tau$, the two subsystems are interactively coupled, with a portion of energy being transferred to the QB. Finally, the interaction is switched off at time $t = \tau$, and the QB is thereby properly charged as intended.

many-body systems. flux qubits (FQs), implemented via superconducting quantum circuits, are based on Josephson junctions.[37,38] In experiments, they exhibit low decay rates and long coherent times on the order of microseconds[39,40] and enable more convenient coherent control.[41,42]

Given the importance of an ideal QB and the availability of superconducting quantum circuits, in this work, we propose such a QB constituted by a series of non-interacting two-level FQs embedded in a single one-dimensional transmission line resonator and collectively coupled to a common photonic mode. Here, we investigate energy manipulation and shed light on the charging performance of QB. By rigorously deriving key figures of merit, we show that the battery can be properly charged in the strong-coupling regime. We then reveal a trade-off relation: increasing the battery size enhances the charging power but suppresses the energy storage capacity. This trade-off relation may originate from the time-energy uncertainty relation, which is known as the quantum speed limit for the minimal evolution time between an initial state and a target state.[43] By choosing an appropriate battery size, we identify a route toward a practical QB that simultaneously achieves high power and large capacity. Moreover, this optimal battery size can be moderately increased by slightly reducing the coupling strength between the FQs and the resonator.

The overall structure of this work is organized as follows. In Sec. II, based on superconducting FQs, we present a general framework for designing a scalable QB and introduce several figures of merit to characterize its charging performances. In Sec. III, we utilize a set of non-interacting FQs to realize a QB engineered within a transmission line resonator and investigate its charging dynamics. Finally, Sec. IV offers a concise summary and outlines our key conclusions.

II. QUANTUM COHERENCE AND BATTERY MODEL

Quantum coherence, a direct consequence of the quantum superposition principle, is conventionally regarded as an intrinsic property that endows quantum states with the ability to exhibit interference phenomena. For an arbitrary quantum state $|\psi\rangle$, such coherence is attributed to the off diagonal elements of its density matrix ρ with respect to a chosen reference basis $\{|i\rangle\}_{i=1}^{d}$. Specifically, we focus on the geometric quantifier, the l_1 norm of coherence C_{l_1}, which is quantified by[1]

$$C_{l_1}(\rho) = \sum_{i,j,i\neq j} |\rho_{ij}|, \tag{1}$$

where $\rho_{ij}(i \neq j)$ are the off diagonal elements of the density matrix ρ.

The charging process of our battery is schematically illustrated in Fig. 1. This process involves two subsystems: a charger C with a certain input energy, and a battery B initially prepared in the ground state, which are described by the Hamiltonians H_C and H_B, respectively. Specifically, we investigate an exactly solvable model consisting of $1 + N$ two-level FQs resonantly coupled to a single transmission line resonator. In operation, one FQ functions as the charger, and the remaining N non-interacting FQs serve as the battery.

In superconducting quantum circuits,[44,45] a FQ consists of a superconducting loop interrupted by three Josephson junctions. By tuning the magnetic flux Φ_x, a four-level FQ can be engineered. Here, we only consider its two lowest levels, which encode the two logic states. The level $|0\rangle$ is defined as the ground state $|g\rangle$ and the level $|1\rangle$ as the excited state $|e\rangle$. Within the FQ Hilbert space spanned by states $|g\rangle$ and $|e\rangle$, the Hamiltonian of a FQ is given by (with $\hbar = 1$ adopted throughout this work)[46]

$$H_q = \frac{\omega_q}{2}\sigma^z, \tag{2}$$

where ω_q is the energy-level splitting between the ground state $|g\rangle$ and the excited state $|e\rangle$, and σ^z is the Pauli matrix.

During the charging process, all FQs are embedded in a single one-dimensional transmission line resonator, and they interact simultaneously with a common photonic mode, as schematically illustrated in Fig. 2. Under the rotating-wave approximation, the global Hamiltonian of the combined charger-battery system is described as

$$H = \omega_c a^\dagger a + \frac{\omega_q}{2}\sum_{k=0}^{N}\sigma_k^z + \sum_{k=0}^{N} g_k\left(a\sigma_k^+ + a^\dagger\sigma_k^-\right), \tag{3}$$

where $a(a^\dagger)$ annihilates (creates) a cavity photon with frequency ω_c, $\sigma_k^\pm$ denote the raising and lowering spin operators for the kth FQ, and g_k is the coupling strength between the resonator and the kth FQ.

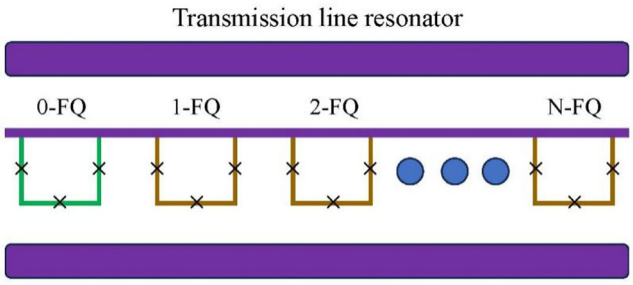

FIG. 2. Schematic diagram of the charger-battery system. The 0-FQ acts as the charger, and the remaining N non-interacting FQs constitute the QB. All FQs are embedded in a single mode transmission line resonator and interact with it simultaneously.

Below, we focus on the total system operating in the dispersive regime, where the coupling strengths g_k are much smaller than the frequency detuning of FQs from the resonator, i.e., $g_k \ll \delta = \omega_c - \omega_q$. Under this condition, the Hamiltonian in Eq. (3) can be decomposed into two parts: a free Hamiltonian and a perturbative term, denoted as $H = H_0 + H_I$. The free Hamiltonian is

$$H_0 = \omega_c a^\dagger a + \frac{\omega_q}{2}\sum_{k=0}^{N}\sigma_k^z, \tag{4}$$

and the perturbation term is

$$H_I = \sum_{k=0}^{N} g_k\left(a\sigma_k^+ + a^\dagger\sigma_k^-\right). \tag{5}$$

To derive the effective Hamiltonian H', we apply the Fröhlich–Nakajima transformation[47,48] to the Hamiltonian given in Eq. (3),

$$H' = UHU^\dagger, \tag{6}$$

where $U = \exp(-V)$ with

$$V = \sum_{k=0}^{N} \eta_k\left(a\sigma_k^+ - a^\dagger\sigma_k^-\right). \tag{7}$$

This V satisfies $[H_0, V] = -H_I$, which gives rise to $\eta_k = g_k/\delta$. Given the small magnitude of the coupling coefficients η_k, the higher-order terms can be neglected, and only the second-order term $[H_I, V]$ needs to be retained in Eq. (6). The effective Hamiltonian H' is, thus, simplified to $H' \simeq H_0 + \frac{1}{2}[H_I, V]$. Utilizing the relations $[\sigma^+, \sigma^-] = \sigma^z$, $[\sigma^z, \sigma^-] = -2\sigma^-$, and $[\sigma^z, \sigma^+] = 2\sigma^+$, we can explicitly express Eq. (6) as[37,49,50]

$$H' = \omega_c' a^\dagger a + \frac{\omega_q'}{2}\sum_{k=0}^{N}\sigma_k^z + \sum_{i\neq j=0}^{N} g_c\left(\sigma_i^+\sigma_j^- + \sigma_i^-\sigma_j^+\right), \tag{8}$$

where

$$\omega_c' = \omega_c - \frac{g^2}{\delta}, \omega_q' = \omega_q - \frac{g^2}{\delta}, g_c = -\frac{g^2}{\delta}. \tag{9}$$

III. CAVITY-MEDIATED CHARGING OF BATTERY

Our battery model consists of N non-interacting two-level FQs, which is described by the Hamiltonian $H_B = \frac{\omega_q}{2}\sum_{k=1}^{N}\sigma_k^z$. Initially, the battery is prepared in the uncharged state $|\psi(0)\rangle_B = |g\rangle^{\otimes N}$, and the charger is initialized in state $|\psi(0)\rangle_C = |e\rangle$. Thus, the total charger-battery system starts from a factorized state $|\psi(0)\rangle_{CB} = |\psi(0)\rangle_C \otimes |\psi(0)\rangle_B$. After an evolution time t, the battery achieves an appropriate charged state, which is obtained by tracing over the charger degrees of freedom from the time-evolved total state $|\psi(t)\rangle_{CB}$. Under the closed-system assumption, the total state satisfies the equation $i\frac{\partial|\psi(t)\rangle_{CB}}{\partial t} = H'|\psi(t)\rangle_{CB}$.[51,52] Subsequently, the density matrix $\rho_B(t)$, which characterizes the charged state of the battery, is derived as

$$\begin{aligned}\rho_B(t) = {} & \xi_1|g^{\otimes N}\rangle\langle g^{\otimes N}| \\ & + \xi_2\begin{bmatrix} |g^{\otimes N-1}e\rangle\langle g^{\otimes N-1}e| + |g^{\otimes N-2}eg\rangle\langle g^{\otimes N-2}eg| + \ldots \\ +|geg^{\otimes N-2}\rangle\langle geg^{\otimes N-2}| + |eg^{\otimes N-1}\rangle\langle eg^{\otimes N-1}| \\ +|g^{\otimes N-1}e\rangle\langle g^{\otimes N-2}eg| + \ldots + |g^{\otimes N-1}e\rangle\langle geg^{\otimes N-2}| \\ +|g^{\otimes N-1}e\rangle\langle eg^{\otimes N-1}| + \ldots + |g^{\otimes N-2}eg\rangle\langle geg^{\otimes N-2}| \\ +|g^{\otimes N-2}eg\rangle\langle eg^{\otimes N-1}| + |geg^{\otimes N-2}\rangle\langle eg^{\otimes N-1}| + H.C.\end{bmatrix},\end{aligned} \tag{10}$$

with $\xi_1 = 1 + \left[\left(\frac{N-1}{N+1}\right)^2 - 1\right]\sin^2\left(\frac{N+1}{2}g_c t\right)$ and $\xi_2 = \frac{4}{(N+1)^2}\sin^2\left(\frac{N+1}{2}g_c t\right)$. According to the definition $C_{l_1}(\rho)$, the coherence is

$$C_{l_1} = \frac{4N(N-1)}{(N+1)^2}\sin^2\left(\frac{N+1}{2}g_c t\right). \tag{11}$$

To evaluate the charging performance, we introduce several figures of merit. First, the energy delivered to the QB system can be characterized by the mean local energy, which is

$$\begin{aligned}E_N(t) &= \mathrm{Tr}[\rho_B(t)H_B] - \langle\psi(0)|H_B|\psi(0)\rangle \\ &= \frac{4N\omega_q}{(N+1)^2}\sin^2\left(\frac{N+1}{2}g_c t\right).\end{aligned} \tag{12}$$

Combining Eqs. (11) and (12), we establish a quantitative relationship between coherence and the mean local energy, yielding $E_N(t) = \frac{\omega_q}{N-1}C_{l_1}$. We also verity that when the battery size is fixed ($N \geq 2$), the intrinsic quantum coherence can effectively facilitate energy transfer.

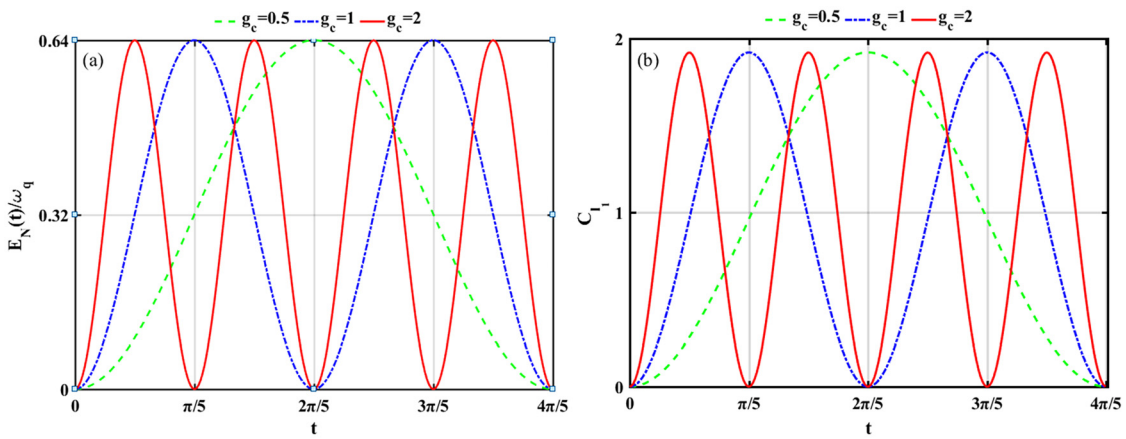

FIG. 3. (a) plots the mean local energy $E_N(t)$ (in unit of ω_q) of a specific QB ($N = 4$) as a function of charging duration t for $g_c = 0.5$ (green dashed line), $g_c = 1$ (blue dash-dotted line), and $g_c = 2$ (red solid line). The corresponding coherence dependence is presented in (b).

As a consequence, the storage capacity is defined as the maximum amount of mean local energy, resulting in

$$C_N = \max_t [E_N(t)] = \frac{4N\omega_q}{(N+1)^2}. \tag{13}$$

By fixing the battery size at a constant value (e.g., $N = 4$), we plot the mean local energy $E_N(t)$ (in units of ω_q) and the coherence as functions of charging duration t for different coupling constants g_c in Fig. 3. Specifically, they are described by a step function that takes a specific value over the interval $[0,\ t]$ and is zero otherwise. As expected, we obtain a striking result that both the evolutionary trends of both the mean local energy and coherence are consistent. They rise to their maximum values and oscillate over time, with all curves exhibiting identical peak values. Physically, these oscillatory phenomena indicate that the transmission line resonator acts as a mediator to induce coherence between battery cells during the charging process, giving rise to Rabi oscillations. It is also shown that the coupling strength has no effect on the storage capacity C_N, which is in good agreement with the result presented in Eq. (13). Interestingly, in the long-time limit, increasing the coupling strength g_c does not enhance the peak energy storage; however, it can significantly reduce the minimum time required to reach the peak energy storage. In other words, the charging power is boosted by the increasing coherence, which demonstrates that strong coupling is beneficial for energy exchange.

We now investigate the role of battery size N in the energy $E_N(t)$, with the corresponding results presented in Fig. 4. As the battery size N increases, both the peak values of the maximum mean local energy and the energy conversion cycle decrease gradually. This reveals a trade-off between charging power and storage capacity; that is, increasing the battery size N effectively enhances the charging power but suppresses the storage capacity. Physically, these dual effects are associated with the coherence generated among the battery subsystems during the charging process. Previous studies have demonstrated that coherence can accelerate the charging process while suppressing energy transfer. This relationship may stem directly from time-energy uncertainty relation, which defines the quantum speed limit for the minimum time between the initial and target states.

Moreover, the charging efficiency described by the average charging power is mathematically quantified as the maximum time-averaged rate of energy transfer into the battery. At the optimal operating stage $t_{op} = 2.331/(N+1)g_c$, the average charging

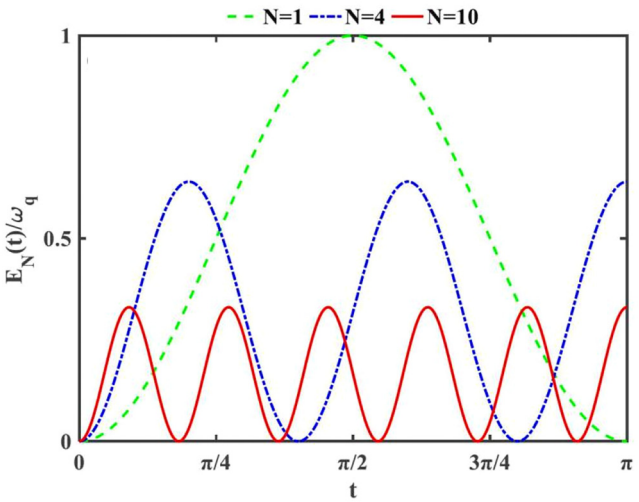

FIG. 4. Dependence of the mean local energy $E_N(t)$ (in unit of ω_q) on battery size N for a coupling strength of $g_c = 1$, with curves for $N = 1$ (green dashed line), $N = 4$ (blue dash-dotted line), and $N = 10$ (red solid line).

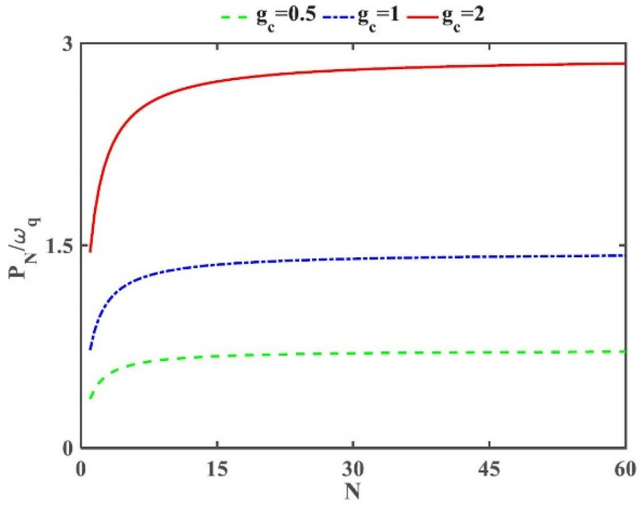

FIG. 5. Charging power P_N (in unit of ω_q) as a function of battery size N for different coupling strengths $g_c = 0.5$ (green dashed line), $g_c = 1$ (blue dash-dotted line), and $g_c = 2$ (red solid line).

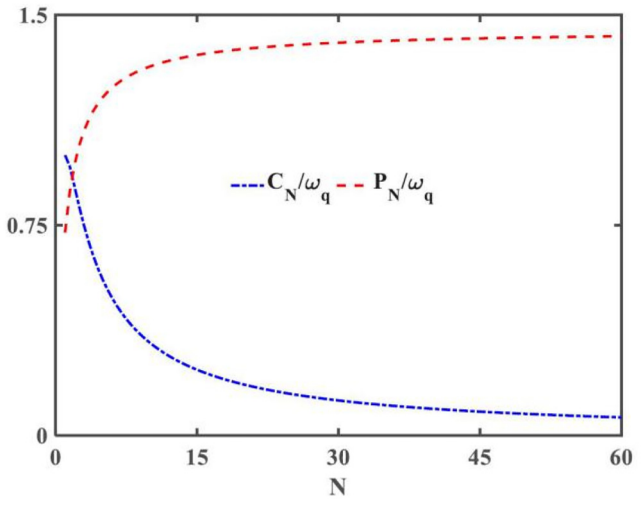

FIG. 6. Stored capacity C_N (blue dashed-dotted line) and charging power P_N (red dashed line) in unit of ω_q as a function of battery size N for the fixed coupling $g_c = 1$.

power is[53,54]

$$P_N = \max_t \left[\frac{E_N(t)}{t}\right] = 1.448\left(\frac{N}{N+1}\right)\omega_q g_c, \tag{14}$$

and exhibits a linear scaling with g_c. Figure 5 plots the charging power as a function of N for different values of the coupling strength g_c. It is clearly observed that the charging power increases with both a stronger coupling strength and a larger battery size. In addition, the charging power rapidly saturates to an asymptotic value as N increases, a trend that holds for all coupling strength values g_c. This indicates that the power P_N reaches a saturation state for sufficiently large values of N. This saturation behavior naturally evokes the corresponding analytical expression $P_N = 1.448[1 - 1/(N+1)]\omega_q g_c$, which converges to $P_N \to 1.448\omega_q g_c$ in the limit of $N \to \infty$.

In practical applications, an ideal QB should simultaneously achieve high power output and large energy capacity during the energy transfer process, which is the so-called cost-effective QB. For a fixed coupling strength $g_c = 1$, the trade-off between charging power and storage capacity as a function of battery size N is depicted in Fig. 6. The results show that the charging power approaches its maximum value only when the storage capacity tends to zero, implying that it is impossible to enhance the power and capacity simultaneously. This finding is in full agreement with the well-established trade-off relationship between resource utilization and energy conversion efficiency in the thermodynamics process. Furthermore, an equilibrium point can be identified where the charging power and storage capacity exhibit equivalent scaling with battery size N^{ce}, which is $N^{ce} = (1 - 0.362g_c)/0.362g_c$. Based on this relationship, a scalable cost-effective QB can be designed by tuning the coupling strength. For instance, to realize a 2-FQ ($N^{ce} = 2$) cost-effective QB, the effective coupling strength should be modulated to approximately $g_c \approx 0.92$. Given the typical values of the coupling parameters discussed in this paper, the experimental realization of the Hamiltonian in Eq. (8) using such a superconducting quantum circuit is feasible. Notably, recent experimental studies have demonstrated the achievement of the strong-coupling $g_c \approx 1$.[55]

IV. CONCLUSIONS

Considering an array of non-interacting two-level FQs, we design a scalable QB integrated within a single one-dimensional transmission line resonator. Mediated by cavity photons, an effective long-range interaction is induced between these FQs, which enables the spontaneous generation of coherence among these battery units during the charging process and, thus, contributes to the enhancement of charging power. In the dispersive regime, we analytically derive a set of figures of merit for characterizing the reliability of the QB, with the aim of developing a fast-charging and high-precision quantum battery system. We uncover a remarkable trade-off between charging power and storage capacity: at a fixed coupling strength, higher power is attained at the expense of reduced storage capacity. Furthermore, a cost-effective QB with both high charging power and large storage capacity can be realized by dynamically tuning the coupling strength g_c, and its physical dimension N^{ce} satisfies the relation $N^{ce} = (1 - 0.362g_c)/0.362g_c$. Our findings yield deeper insights into the fundamental properties of quantum resource-driven dispersive QBs and pave a viable pathway for the design of more efficient and controllable quantum energy storage devices.

ACKNOWLEDGMENTS

This work was supported by the National Science Foundation of China (NSFC) under Grant No. 12205047, the Key Project for

Cultivating Outstanding Young Teachers in the Training Program for Middle-aged and Young Teachers in Anhui Province under Grant No. YQZD2025094, the Natural Science Research Project of Education Department of Anhui Province of China under Grant No. 2022AH040199, the Anhui Provincial Natural Science Foundation under Grant No. 2308085QF195, and also the Talent Foundation of Hefei Institute of Technology under Grant Nos. 2025KY04, 2025KY05, and 2025KY07.

AUTHOR DECLARATIONS

Conflict of Interest

The authors have no conflicts to disclose.

Author Contributions

Jiadong Shi: Formal analysis (equal); Investigation (lead); Writing – original draft (lead). **Jiaxu Wu:** Investigation (supporting); Software (lead). **Tao Wu:** Formal analysis (equal); Investigation (supporting); Writing – review & editing (lead).

DATA AVAILABILITY

The data that support the findings of this study are available within the article.

REFERENCES

[1]T. Baumgratz, M. Cramer, and M. B. Plenio, Phys. Rev. Lett. **113**, 140401 (2014).
[2]F. Campaioli, F. A. Pollock, F. C. Binder *et al.*, Phys. Rev. Lett. **118**, 150601 (2017).
[3]P. Faist, M. Berta, and F. Brandão, Phys. Rev. Lett. **122**, 200601 (2019).
[4]C. A. Vincent and B. Scrosati, *Modern Batteries: An Introduction to Electrochemical Power Sources* (Arnold, 1997), p. 351.
[5]M. N. Bera, A. Riera, M. Lewenstein *et al.*, Nat. Commun. **8**, 2180 (2017).
[6]H. Kwon, H. Jeong, D. Jennings *et al.*, Phys. Rev. Lett. **120**, 150602 (2018).
[7]G. Vitagliano, C. Klockl, M. Huber *et al.*, "Trade-off between work and correlations in quantum thermodynamics," *Thermodynamics in the Quantum Regime*: *Fundamental Aspects and New Directions*, edited by F. Binder, L. A. Correa, C. Gogolin *et al.* (Springer, 2019), pp. 731–750.
[8]B. Morris, L. Lami, and G. Adesso, Phys. Rev. Lett. **122**, 130601 (2019).
[9]K. Korzekwa, C. T. Chubb, and M. Tomamichel, Phys. Rev. Lett. **122**, 110403 (2019).
[10]S. Deffner and S. Campbell, J. Phys. A **50**, 453001 (2017).
[11]C. Perry, P. Cwiklinski, J. Anders *et al.*, Phys. Rev. X **8**, 041049 (2018).
[12]P. Mazurek and M. Horodecki, New J. Phys. **20**, 053040 (2018).
[13]M. Lostaglio, A. M. Alhambra, and C. Perry, Quantum **2**, 52 (2018).
[14]H. Xu, X. K. Song, D. Wang, and L. Ye, Sci. China-Phys. Mech. Astron. **66**, 240314 (2023).
[15]X. K. Song, H. Zhang, Q. Ai *et al.*, New J. Phys. **18**, 023001 (2016).
[16]R. Alicki and M. Fannes, Phys. Rev. E **87**, 042123 (2013).
[17]P. R. Lai, J. D. Lin, Y. T. Huang *et al.*, Phys. Rev. Res. **6**, 023136 (2024).
[18]T. F. F. Santos, Y. V. de Almeida, and M. F. Santos, Phys. Rev. A **107**, 032203 (2023).
[19]D. Rossini, G. M. Andolina, D. Rosa *et al.*, Phys. Rev. Lett. **125**, 236402 (2020).
[20]M. L. Hu, T. Gao, and H. Fan, Phys. Rev. A **111**, 042216 (2025).
[21]Y. Yao and X. Q. Shao, Phys. Rev. A **111**, 062616 (2025).
[22]M. L. Song, X. K. Song, L. Ye, and D. Wang, Phys. Rev. E **109**, 064103 (2024).
[23]M. L. Song, L. J. Li, X. K. Song *et al.*, Phys. Rev. E **106**, 054107 (2022).
[24]Z. G. Lu, G. Q. Tian, X. Y. Lü, and C. Shang, Phys. Rev. Lett. **134**, 180401 (2025).
[25]B. Ahmadi, P. Mazurek, P. Horodecki *et al.*, Phys. Rev. Lett. **132**, 210402 (2024).
[26]X. L. Zhang, X. K. Song, and D. Wang, Adv. Quantum Technol. **7**, 2400114 (2024).
[27]J. Q. Quach, K. E. McGhee, L. Ganzer *et al.*, Sci. Adv. **8**, eabk3160 (2022).
[28]H. Y. Yang, H. L. Shi, Q. K. Wan *et al.*, Phys. Rev. A **109**, 012204 (2024).
[29]A. Canzio, V. Cavina, M. Polini *et al.*, Phys. Rev. A **11**, 022222 (2025).
[30]C. K. Hu, J. Qiu, P. J. P. Souza *et al.*, Quantum Sci. Technol. **7**, 045018 (2022).
[31]I. M. de Buy Wenniger S. E. Thomas *et al.*, Phys. Rev. Lett. **131**, 260401 (2023).
[32]J. Joshi and T. S. Mahesh, Phys. Rev. A **106**, 042601 (2022).
[33]J. Q. You, J. S. Tsai, and F. Nori, Phys. Rev. Lett. **89**, 197902 (2002).
[34]J. Q. You, X. D. Hu, S. Ashhab *et al.*, Phys. Rev. B **75**, 140515(R) (2007).
[35]C. Song, K. Xu, H. K. Li *et al.*, Science **365**, 574–577 (2019).
[36]X. T. Wu, H. X. Yan, G. Andersson *et al.*, Phys. Rev. X **14**, 041030 (2024).
[37]W. Xiong, D. Y. Jin, J. Jing *et al.*, Phys. Rev. A **92**, 032318 (2015).
[38]Z. L. Xiang, S. Ashhab, J. Q. You *et al.*, Rev. Mod. Phys **85**, 623 (2013).
[39]L. B. Nguyen, Y. H. Lin, A. Somoro *et al.*, Phys. Rev. X **9**, 041041 (2019).
[40]A. D. O'Connell M. Hofheinz *et al.*, Nature **464**, 697 (2010).
[41]X. S. Tan, D. W. Zhang, Z. Yang *et al.*, Phys. Rev. Lett. **122**, 210401 (2019).
[42]J. Z. Lin, K. Hou, C. J. Zhu *et al.*, Phys. Rev. A **99**, 053850 (2019).
[43]V. Giovannetti, S. Lloyd, and L. Maccone, J. Opt. B: Quantum Semiclassical Opt. **6**, S807 (2004).
[44]J. E. Mooij, T. P. Orlando, L. Levitov *et al.*, Science **285**, 1036 (1999).
[45]X. L. He, C. P. Yang, S. Li *et al.*, Phys. Rev. A **82**, 024301 (2010).
[46]Z. R. Zhang, C. Y. Li, C. W. Wu *et al.*, Phys. Rev. A **88**, 044303 (2013).
[47]H. Fröhlich, Phys. Rev **79**, 845 (1950).
[48]S. Nakajima, Adv. Phys **4**, 363 (1955).
[49]G. P. Guo, C. F. Li, J. Li, and G. C. Guo, Phys. Rev. A **65**, 042102 (2002).
[50]E. Buks, P. Brookes, E. Ginossar *et al.*, Phys. Rev. A **102**, 043716 (2020).
[51]W. L. Yang, Z. Q. Yin, Y. Hu *et al.*, Phys. Rev. A **84**, 010301(R) (2011).
[52]H. R. Wei and G. L. Long, Phys. Rev. A **91**, 032324 (2015).
[53]F. C. Binder, S. Vinjanampathy, K. Modi *et al.*, New J. Phys. **17**, 075015 (2015).
[54]D. Ferraro, M. Campisi, G. M. Andolina *et al.*, Phys. Rev. Lett. **120**, 117702 (2018).
[55]F. Yoshihara, T. Fuse, S. Ashhab *et al.*, Nat. Phys. **13**, 44 (2017).